Molecular Cell, Vol. 7, 1153–1163, June, 2001, Copyright ©2001 by Cell Press

Diabetes Mellitus and Exocrine Pancreatic Dysfunction in *Perk*−/− Mice Reveals a Role for Translational Control in Secretory Cell Survival

Heather P. Harding,[1] Huiqing Zeng,[1] Yuhong Zhang,[1] Rivka Jungries,[1] Peter Chung,[1] Heidi Plesken,[2] David D. Sabatini,[2] and David Ron[1,2,3,4,5]
[1] Skirball Institute of Biomolecular Medicine
[2] Department of Cell Biology
[3] Department of Medicine
[4] Kaplan Cancer Center
New York University School of Medicine
New York, New York 10016

Summary

The protein kinase PERK couples protein folding in the endoplasmic reticulum (ER) to polypeptide biosynthesis by phosphorylating the α subunit of eukaryotic translation initiation factor 2 (eIF2α), attenuating translation initiation in response to ER stress. PERK is highly expressed in mouse pancreas, an organ active in protein secretion. Under physiological conditions, PERK was partially activated, accounting for much of the phosphorylated eIF2α in the pancreas. The exocrine and endocrine pancreas developed normally in *Perk*−/− mice. Postnatally, ER distention and activation of the ER stress transducer IRE1α accompanied increased cell death and led to progressive diabetes mellitus and exocrine pancreatic insufficiency. These findings suggest a special role for translational control in protecting secretory cells from ER stress.

Introduction

All eukaryotic cells have signaling pathways that monitor the folding environment in the endoplasmic reticulum (ER) and respond to the accumulation of malfolded proteins in the organelle. This is referred to as the unfolded protein response (UPR), and has two main components, one transcriptional and the other translational. The first alters gene expression patterns and accounts for the increased synthesis of ER chaperones and components of the apparatus that degrades proteins retained in the ER. The second attenuates polypeptide biosynthesis and is presumed to decrease the level of protein malfolding in the organelle by reducing the load placed on it by the biosynthetic machinery (reviewed in Kaufman, 1999; Mori, 2000).

Translational repression in the UPR is associated with phosphorylation of the α subunit of eukaryotic translation initiation factor 2 (eIF2α) on Ser51 (Kimball and Jefferson, 1992; Prostko et al., 1992, 1993). Phosphorylation of eIF2α on Ser51 increases its affinity for the guanine nucleotide exchange factor, eIF2B, and sequesters the latter in an inactive complex. Reduced eIF2B activity prevents the regeneration of active eIF2 complexes and attenuates translation initiation (Clemens, 1996). Various cellular stress pathways converge on this common step to control polypeptide biosynthesis rates. These stress pathways utilize specific eIF2α kinases to affect this goal. For example, PKR responds to the accumulation of double-stranded RNA during viral infection, GCN2 responds to uncharged tRNA in nutrient-deprived cells, and HRI matches the biosynthesis of globin to the availability of its essential prosthetic group, heme (reviewed in Clemens, 1996).

PERK (*P*KR-like *ER k*inase) is a recently identified transmembrane eIF2α kinase that resides in the ER and couples stress signals initiated by protein malfolding in the ER lumen to eIF2α phosphorylation and reduced protein biosynthesis (Harding et al., 1999; Bertolotti et al., 2000; Sood et al., 2000). *Perk*−/− cells are unable to phosphorylate eIF2α and attenuate translation in response to ER stress (Harding et al., 2000b). The absence of PERK also renders cultured cells hypersensitive to toxins that impair protein folding in the ER. When exposed to such toxins, *Perk*−/− cells exhibit higher levels of activation of parallel ER stress pathways, indicating that the mutant cells experience more ER stress than do wild-type cells (Harding et al., 2000b). These results established the essential role of PERK in the response of mammalian cells to pharmacologically induced ER stress and suggested that translational control is an important component of that response. However, the studies described above were carried out in cultured cells exposed to pharmacological agents that cause ER stress, and did not inform us of the significance of translational control under physiological circumstances. Here, we present a phenotypic characterization of *Perk*−/− mice that reveals an important role for PERK-mediated translational control in the adaptation of secretory cells to the physiological loads of protein biosynthesis.

Results

PERK (also known as *PEK*) has been independently isolated as a gene encoding an eIF2α kinase that is expressed at high levels in the pancreas (Shi et al., 1998; Sood et al., 2000). We confirmed the abundance of PERK in the pancreas by immunohistochemistry that revealed the protein in both the acini that produce and secrete digestive enzymes and the islets of Langerhans, which produce and secrete the polypeptide hormones insulin and glucagon (Figure 1A). In exocrine acinar cells, PERK immunoreactivity was found concentrated in the basolateral portion of the cell, consistent with the known localization of the ER in these cells (Pictet et al., 1972). Immunostaining of pancreatic sections of *Perk*−/− mice revealed no signal, attesting to the specificity of the staining procedure.

Immunoprecipitation and immunoblotting detected different levels of PERK protein in various mouse tissues (Figure 1B), and no PERK signal was detected in tissues from *Perk*−/− mice (Figure 1C). When PERK is activated, it undergoes autophosphorylation, which can be detected both by a shift in the mobility of the protein on SDS-PAGE (Harding et al., 1999) and by reactivity of

[5] Correspondence: ron@saturn.med.nyu.edu

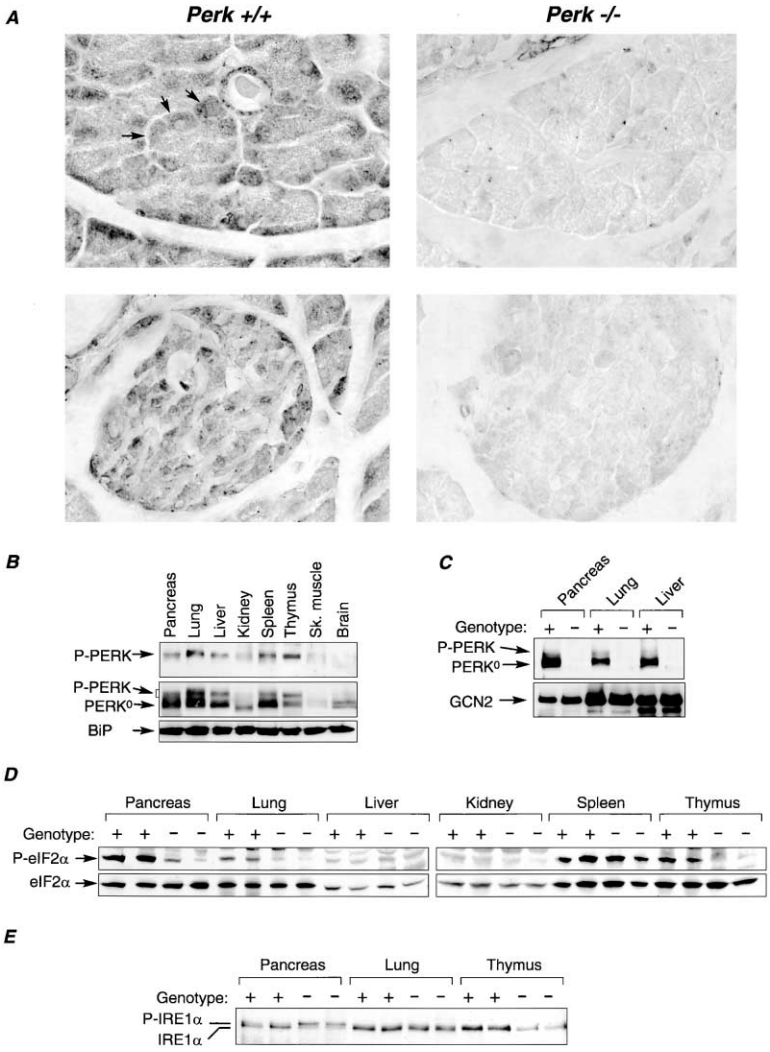

Figure 1. PERK Controls eIF2α Phosphorylation Levels in the Pancreas under Physiological Conditions

(A) Anti-PERK immunostaining of paraffin-embedded sections of pancreatic acini (upper panels) and islets of Langerhans (lower panel). The arrows point to the basolateral distribution of PERK immunoreactivity in the cells of the acinus.

(B) Total PERK (middle panel) and activated, phosphorylated PERK (upper panel) were detected by immunoblot with specific antiserum in immunoprecipitates of tissue extracts of wild-type mice. The positions of inactive PERK ($PERK^0$) and the slower migrating active form of the protein (P-PERK) are indicated. BiP immunoblot from 0.75% of the lysate used in the immunoprecipitation provides a means for comparing ER content in the different lysates (lower panel).

(C) Immunoblot of PERK immunoprecipitated from tissue extracts of *Perk*+/+ (+) and *Perk*−/− mice (−; upper panel). Immunoblot of GCN2, immunoprecipitated from the same lysates reports on their comparability (lower panel).

(D) Immunoblot of eIF2α phosphorylated on Ser51 and total eIF2α in tissue lysates from two mice with *Perk*+/+ (+) and two mice with *Perk*−/− genotypes (−).

(E) Immunoblot of IRE1α immunoprecipitated from lysates of mice as in (D). The positions of inactive IRE1α and the slower migrating active form (P-IRE1α) are indicated.

the activated, phosphorylated form of the protein with specific antisera (Bertolotti et al., 2000). Based on both criteria, PERK was active in many mouse tissues, suggesting that signaling through the PERK pathway occurs under physiological conditions (Figures 1B and 1C).

To determine whether under physiological conditions PERK activity correlated with eIF2α phosphorylation on Ser51, we used an antiserum that specifically detects the phosphorylated form of eIF2α to compare, by immunoblot, the ratio of phosphorylated to total eIF2α in tissues of wild-type and *Perk*−/− mice. The ratio of phosphorylated to total eIF2α was significantly reduced in the pancreas, lung, and thymus of *Perk*−/− mice, whereas in other tissues, such as the liver and spleen, there were no detectable differences between the ratio in wild-type and mutant animals (Figure 1D). These results indicate that PERK plays an important role in phosphorylating eIF2α, and may modulate translation in the pancreas and other tissues under physiological conditions. Other kinases such as GCN2 and PKR may account for residual levels of eIF2α phosphorylation in *Perk*−/− tissues.

If PERK is active under physiological conditions, one might expect that the absence of PERK would result in higher levels of ER stress. This might be predicted to increase signaling through parallel, PERK-independent ER stress pathways in tissues of *Perk*−/− mice. IRE1α is a ubiquitous transmembrane ER resident protein kinase that responds to the same stress signals as PERK (Tirasophon et al., 1998; Bertolotti et al., 2000; Liu et al., 2000). Activation of IRE1α also correlates with its autophosphorylation and shift in mobility on SDS-PAGE (Bertolotti et al., 2000; Urano et al., 2000). Activation of IRE1α was markedly increased in the pancreas of *Perk*−/− mice, consistent with higher levels of ER stress in that tissue (Figure 1E).

To examine the phenotypic consequences of reduced eIF2α phosphorylation and the presumed defect in translational regulation in the pancreas of *Perk*−/− mice, we studied the control of blood glucose, which depends on the ability of the endocrine portion of the pancreas to secrete insulin appropriately. Between birth and 4 weeks of age, the *Perk*−/− mice experienced a marked deterioration in glycemic control. Before 2 weeks of age, most *Perk*−/− animals had random blood glucose levels that were within the normal range for suckling mice. After 4 weeks of age, all of the *Perk*−/− animals had markedly elevated blood glucose levels

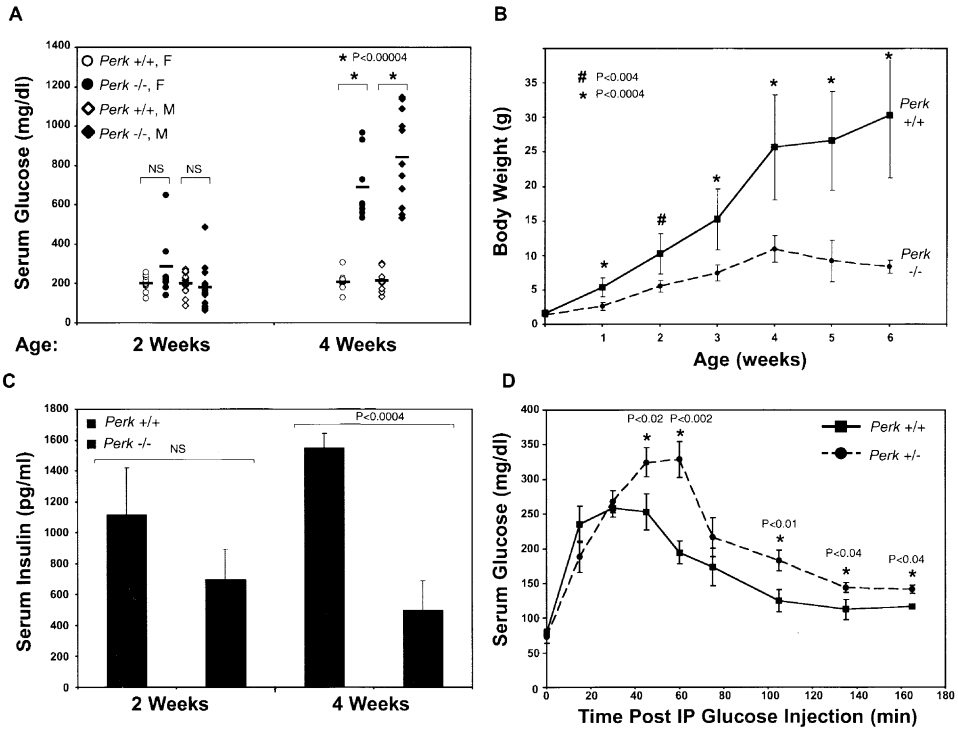

Figure 2. Hyperglycemia and Reduced Serum Insulin Levels in *Perk* Mutant Mice

(A) Spot blood glucose levels in *Perk*+/+ and *Perk*−/− littermates obtained at 2 and 4 weeks of age. The data is analyzed separately for males (diamonds) and females (circles). Horizontal bars mark the mean for each group. (2 weeks: females, n = 8; males, n = 13; 4 weeks: females, n = 8; males, n = 11).

(B) Body weight plotted against age in a cohort of *Perk*+/+ and *Perk*−/− male littermates (n = 10).

(C) Serum insulin levels in male mice of the indicated genotype and age. Shown are means and SEM (n = 8).

(D) Blood glucose levels following intraperitoneal injection of glucose (2 mg/g body weight) into fasted adult male *Perk*+/+ and *Perk*+/− siblings. Shown are means and SD (n = 5). P values for significantly different pairwise comparisons are indicated.

(Figure 2A). The *Perk*−/− animals had significantly lower body weights than wild-type littermates (Figure 2B), and serum insulin levels were reduced in the *Perk*−/− animals (Figure 2C). These results indicate that the hyperglycemia in *Perk*−/− mice was due primarily to the failure of the endocrine pancreas to secrete adequate amounts of insulin and not as a consequence of peripheral resistance to the action of the hormone.

We also compared blood glucose levels in wild-type and *Perk*+/− adult male mice following an intraperitoneal glucose injection. Wild-type mice cleared the glucose load more rapidly that the heterozygous mutant mice, indicating a mild defect in glycemic control in the *Perk*+/− mice (Figure 2D). This defect was observed in two isogenic strain backgrounds (129svev and F1 hybrids of 129svev and C57B/6), was stable over 26 weeks of observation, and did not lead to fasting hyperglycemia (data not shown). The reduced ability of *Perk*+/− mice to clear a glucose load is consistent with a mild haploid insufficiency phenotype of the *Perk* mutation that is also reflected in impaired eIF2α phosphorylation in cultured *Perk*+/− cells exposed to agents that cause ER stress (Harding et al., 2000b). Furthermore, while the *Perk*−/− mice had a complex phenotype that included exocrine pancreatic insufficiency (see Figure 5), growth retardation (Figure 2B), and high mortality, the *Perk*+/− mice were indistinguishable from wild-type littermates in weight and longevity. Therefore, the defect in glycemic control observed in the *Perk*+/− animals was unlikely to have been secondary to other pleotrophic effects of the mutation and supports a primary site of action of the gene in the endocrine pancreas.

To examine the anatomic basis for the defect in glycemic control of *Perk*−/− mice, we stained pancreatic sections with antisera to insulin and glucagon, the major polypeptide hormones produced by the endocrine pancreas. At postnatal day 12, *Perk*−/− mice had normal-appearing islets of Langerhans, with a thin mantle of glucagon-producing cells surrounding a large core of insulin-producing cells. With time, however, the size of the islets decreased, the mass of insulin-producing cells diminished, and the proportion of glucagon-positive cells increased, and they were found to populate the core of the islet as well as its mantle (Figure 3A). The loss of cells that were immunoreactive with the insulin antisera correlated with the loss of cells reactive with an insulin cRNA in situ histohybridization probe (Figure 3B). The latter indicates that the loss of insulin-positive cells was not due to the depletion of insulin stores, but rather to the progressive loss of cells capable of synthesizing the hormone.

Perk−/− cells are more prone to programmed cell death when exposed in culture to conditions that promote protein malfolding in the ER (Harding et al., 2000b).

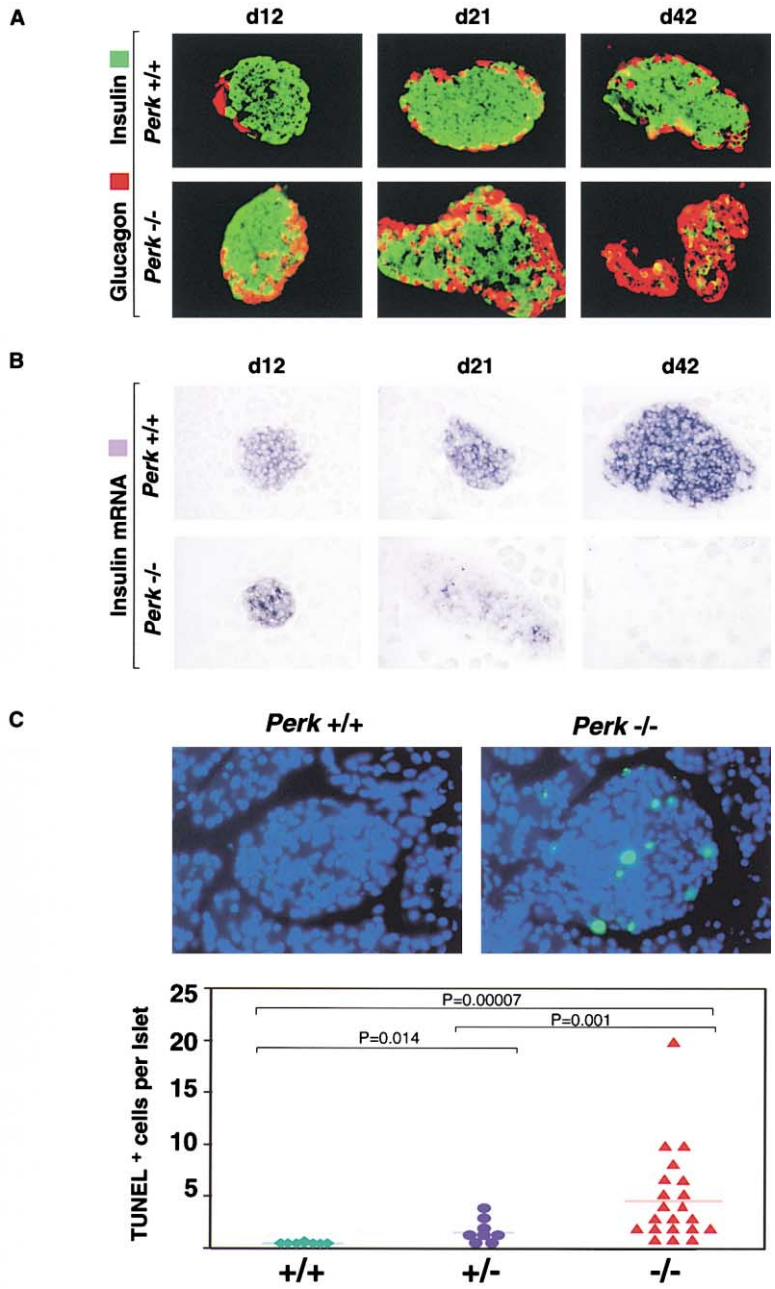

Figure 3. Progressive Loss of Insulin-Producing β Cells in the Islets of Langerhans of *Perk*−/− Mice

(A) Insulin and glucagon immunostaining of cells in islets of *Perk*+/+ and *Perk*−/− mice of the indicated age.

(B) Insulin mRNA detected by in situ histohybridization in the same section shown in (A).

(C) Programmed cell death in islets, detected by TUNEL labeling in 15-day-old *Perk*+/+ and *Perk*−/− mice. The TUNEL-positive cells are detected by the FITC tag (green), and nuclei of all cells react with the karyophilic dye H3328 (blue). The lower panel shows the average number of TUNEL-positive cells per islet in individual mice of the indicated genotype. The horizontal bar is the group mean. P values were determined by a two-tailed t test.

To examine the role of programmed cell death in the loss of insulin-positive cells in the *Perk*−/− islets, we measured the number of TUNEL-positive cells in paraffin-embedded sections of wild-type, *Perk*+/−, and *Perk*−/− pancreas. An average of 4.54 such cells per islet were observed in the *Perk*−/− mice. The location of the TUNEL-positive cells in the center of the islet suggests that they are insulin-producing cells. The *Perk*+/− mice had 1.36 TUNEL-positive cells per islet, compared with 0.19 cells per islet in *Perk*+/+ mice (Figure 3C). These results suggest that increased cell death plays an important role in the progressive destruction of the insulin-producing cell mass in mutant mice.

Insulin mRNA translation and protein biosynthesis as well as total protein biosynthesis are upregulated by extracellular glucose levels (Itoh and Okamoto, 1980; Skelly et al., 1996). To determine whether PERK plays a role in this regulation, we explanted islets of Langerhans from prediabetic 12-day-old *Perk*+/+ and *Perk*−/− littermates and compared insulin biosynthesis by pulse labeling after culture at 2.8 mM glucose and 16.7 mM glucose. Insulin biosynthesis was suppressed by culturing islets of both genotypes at low glucose and was markedly enhanced by switching to media with a high concentration of glucose (Figures 4A and 4B). These results indicate that PERK is not required for the suppression of insulin biosynthesis at low glucose levels. The notable difference between wild-type and mutant islets was the higher level of insulin biosynthesis in the mutant islets. This finding suggests that PERK activity

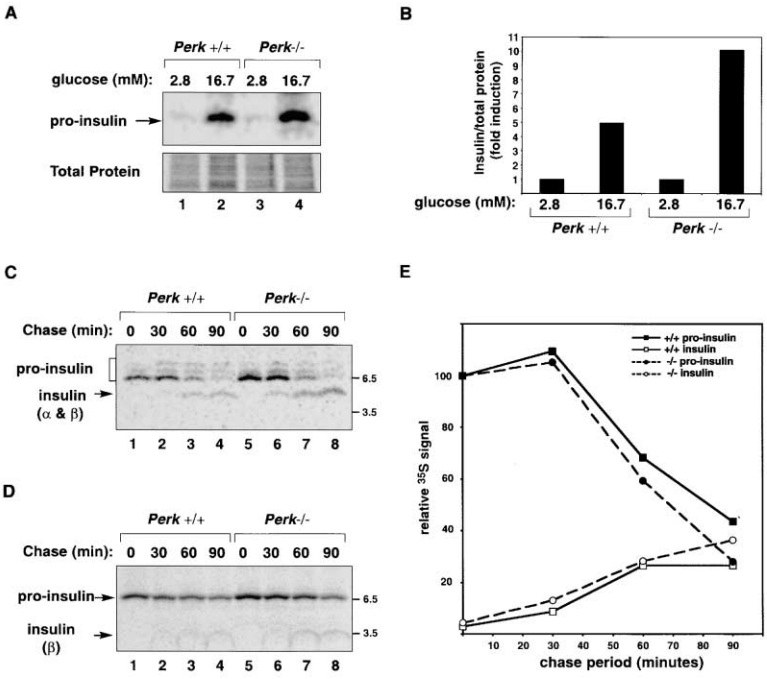

Figure 4. Increased Glucose-Induced Proinsulin Biosynthesis and Normal Processing of Proinsulin in Islets of Langerhans Isolated from Prediabetic *Perk*−/− Mice

(A) Autoradiograph of metabolically labeled proinsulin immunoprecipitated with a C peptide antibody from islets isolated from *Perk*+/+ and *Perk*−/− mice (upper panel) or total protein extracted prior to immunoprecipitation (lower panel; a control). The islets were cultured at 2.8 or 16.7 mM glucose for 40 min before pulse labeling for 20 min with [^{35}S]methionine.

(B) Bar diagram of the fold change in the ratio of insulin biosynthesis to total protein biosynthesis in *Perk*+/+ and *Perk*−/− islets.

(C) Autoradiogram of metabolically labeled proinsulin and insulin immunoprecipitated from islets isolated from *Perk*+/+ and *Perk*−/− mice with both C peptide antibody and an antibody that recognizes mature insulin. Labeled proteins were resolved by PAGE under nonreducing conditions. The labeled proinsulin and mature insulin were immunoprecipitated immediately after a 20 min pulse or following a cold chase of the indicated time. The migration of proinsulin and mature insulin is indicated.

(D) Autoradiogram of metabolically labeled proteins as in (C), resolved under reducing conditions. The migration of proinsulin and the β chain of mature insulin are indicated (the α chain is not revealed on this gel).

(E) Quantitation of the proinsulin and mature insulin signals shown in (C).

attenuates the normal increase in insulin translation in islet cells responding to a carbohydrate load. Since serum insulin levels are tightly regulated at the level of hormone secretion, it is not surprising that the increased biosynthesis of insulin demonstrated here does not translate into higher serum levels in the prediabetic mutant mice. We note that the PERK mutation preferentially affects insulin biosynthesis over total protein biosynthesis (Figure 4A, lower panel). This is consistent with the possibility of selective modulation of translation in membrane-bound ribosomes by PERK.

To address the role of the *Perk* mutation on the processing and maturation of newly synthesized insulin, we performed pulse-chase analysis of metabolically labeled wild-type and *Perk*−/− islets. To enhance the potential effect of the *Perk* mutation, we increased the load on the ER by performing both the pulse labeling and the chase in high (16.7 mM) glucose. As expected, insulin biosynthesis was greater in the *Perk*−/− islets. However, the rates of proinsulin clearance from the ER (revealed by immunoprecipitation with an antiserum to the C peptide) and the rate of production of processed α and β chain dimers (immunoprecipitated with an antibody to the mature hormone) were not measurably different in the two genotypes (Figures 4C–4E). In both genotypes, less than 40% of the radiolabeled signal originally present in proinsulin was converted to mature insulin. We attributed this to the higher immunoprecipitating efficiency of the anti-C peptide antiserum, compared with the antiserum directed against the mature hormone. The amount of label that was recovered as processed insulin is even lower in the reducing gel in which the α chain, which contains 2/3 of the labeled residues, is not retained (Figure 4D). The similar rates of conversion of proinsulin to insulin in the two genotypes indicated that ER and post-ER processing of insulin was normal in *Perk*−/− mice, and argues against a general defect of ER function in the mutant islets.

The exocrine portion of the pancreas contributes to more that 95% of its mass. PERK activation in wild-type mice and reduced eIF2α phosphorylation in pancreatic tissue extracts of mutant mice likely reflected events that took place in exocrine cells (Figures 1B and 1D). This suggested that under physiological conditions, the exocrine pancreas might have the potential for developing ER stress, which is mitigated by the activity of PERK. Therefore, we examined exocrine pancreatic function in mutant mice. Exocrine pancreatic insufficiency results in inadequate secretion of digestive enzymes and incomplete digestion of foodstuffs. One of the earliest and easiest to detect manifestations of pancreatic maldigestion is the presence of intact triglycerides in the stool, or so-called steatorrhea. Wild-type mice are able to digest virtually all the fat in a 45% fat diet, and stool smears from wild-type mice stained with Oil Red O show very few if any red-staining lipid globules. By contrast, the stool of *Perk*−/− mice fed the same diet was visibly greasy, and staining with Oil Red O revealed abundant lipid droplets (Figure 5A). The exocrine portions of the pancreas of *Perk*−/− mice had many TUNEL-positive cells, whereas few were seen in the pancreas of age-matched wild-type littermates (Fig-

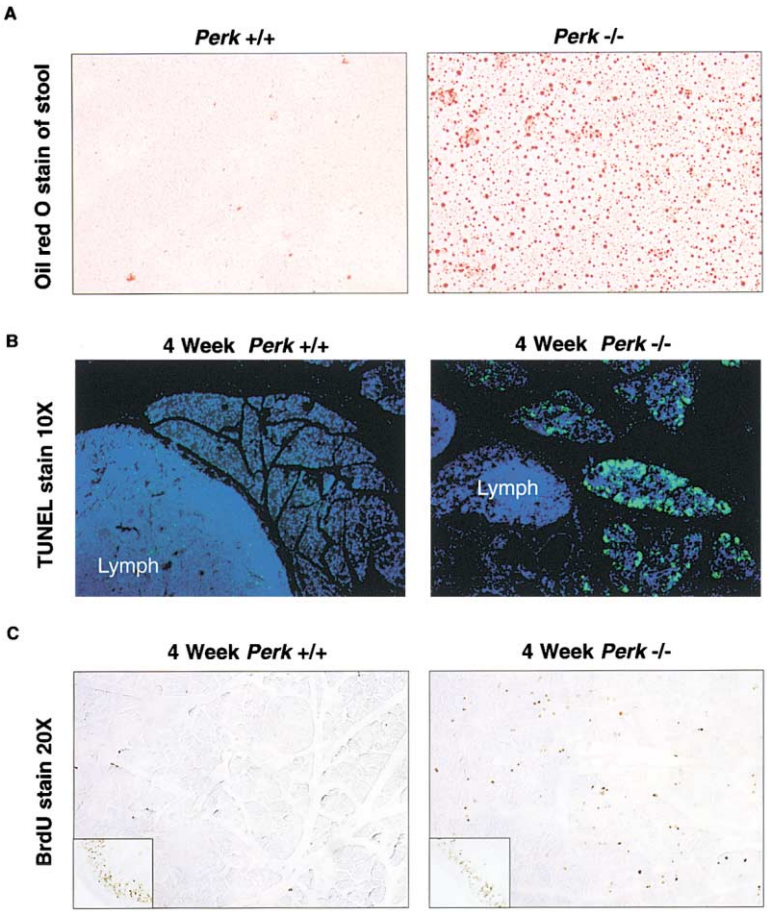

Figure 5. Exocrine Pancreatic Insufficiency in *Perk*−/− Mice

(A) Stool smears of *Perk*+/+ and *Perk*−/− mice stained with Oil Red O. Note the presence of the large number of undigested lipid droplets staining red in the stool of the mutant animal, indicative of maldigestion.

(B) Low-magnification view of TUNEL staining of acinar tissue of *Perk*+/+ and *Perk*−/− mice The TUNEL-positive cells are detected by the FITC tag (green) and nuclei of all cells react with the karyophilic dye H3328 (blue). The positive cells in the lymph node in both samples serve as an internal control for the TUNEL stain.

(C) BrdU incorporation into acinar cells following injection of BrdU into *Perk*−/− and control *Perk*+/− mice, revealed by staining with a monoclonal antibody to BrdU. The presence of the expected labeling of intestinal crypt cells with BrdU in both genotypes (inset) serves as an internal control for the injection and incorporation of the tracer.

ure 5B). Ongoing cell death in the exocrine pancreas of the mutant mice was also associated with evidence for cellular regeneration, reflected in the abundance of cells that incorporated BrdU into replicating DNA following in vivo injection (Figure 5C). Together, these findings are consistent with a role for *Perk* in preserving the integrity of the acinar cells of the exocrine pancreas.

The known role of PERK as a modulator of translation and evidence presented here for increased levels of ER stress in *Perk*−/− pancreas (Figure 1D) led us to examine whether the mutation was associated with ultrastructural abnormalities in the ER. Electron micrographs of islets of Langerhans in pancreases obtained from prediabetic *Perk*−/− animals revealed that most endocrine pancreatic cells had normal morphology (data not shown). However, in islets of all mutant animals examined, occasional cells with striking, abundant, and dilated membrane-bounded cisterna filled with a dense content were observed (Figures 6B–6D). These cells generally had considerably fewer secretory granules than the normal counterparts in the same islet. We screened through multiple sections of age-matched wild-type littermates and never observed a similar cell. In many instances, it was clear that the dilated cisterna was continuous with the perinuclear cisterna, which was similarly filled with a dense content (Figures 6B and 6C). These features indicate that the striking, dilated structures represent abnormal ER cisterna. The abundant amorphous material filling the distended lumen of the cisterna was clearly of much higher electron density than the scarce material found normally in the lumen of the ER of endocrine pancreatic cells (Figure 6A).

Cells in the exocrine pancreas of mutant mice also had characteristic abnormalities in their ER. Instead of being organized into long, thin, densely packed cisterna, the ER in many mutant cells (Figure 6F) was segmented and its lumen was distended with material of higher electron density than the contents of normal ER (Figure 6E). Collectively, these observations indicate that the absence of PERK is associated with the abnormal accumulation of lumenal content, most likely improperly folded secretory proteins in the lumen of the ER of cells engaged in protein secretion.

Discussion

Perk−/− mice experience rapid and progressive decline in endocrine and exocrine pancreatic function. The time course to the development of florid hyperglycemia was invariably less than 4 weeks, and exocrine pancreatic insufficiency, though more variable in onset, was observed in most mutant mice by 6–8 weeks of age. Histological analysis and immunochemical marker studies show that both the endocrine and exocrine pancreases develop normally in *Perk*−/− mice and indicate that tissue dysfunction is acquired postnatally.

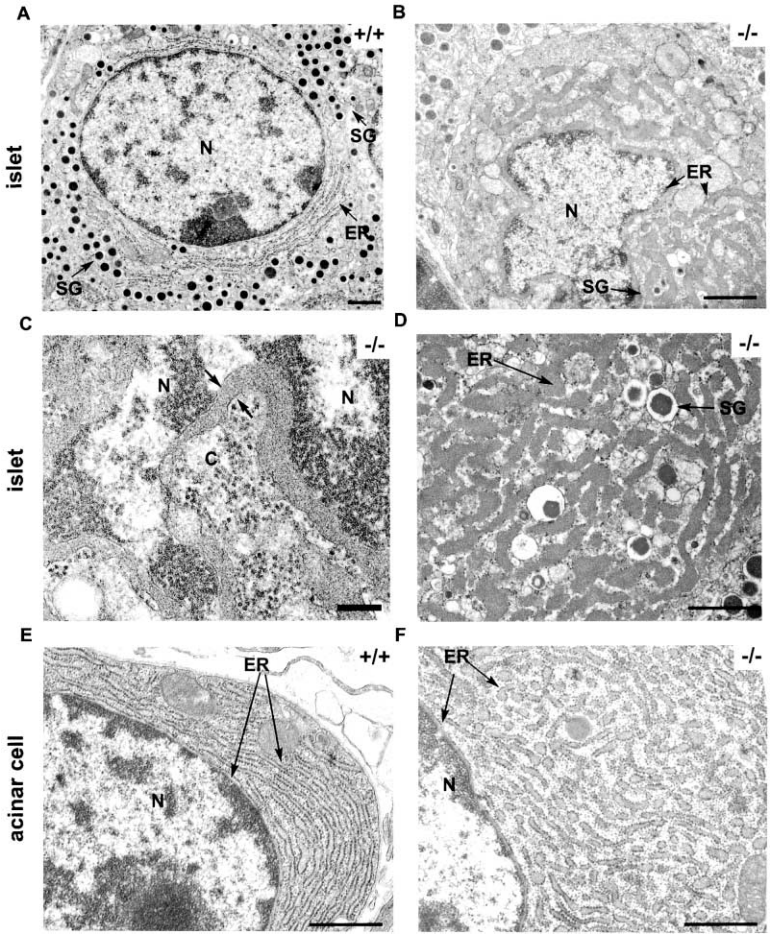

Figure 6. Lumenal Distension and Accumulation of Electron-Dense Material in the Lumen of the ER in *Perk*−/− Pancreatic Cells

(A–D) Electron micrographs of sections of islets from *Perk*+/+ and *Perk*−/− mice. The nucleus is marked "N" and secretory granules are marked "SG;" arrows point to the ER. Note the dilated ER and perinuclear cisterna filled with electron-dense material in (B) and compare with the normal structure in (A). The arrows in (C) point to membranes on opposing sides of the dilated perinuclear cisterna in a mutant cell. The cells shown in (B–D) are from different *Perk*−/− animals and are representative of similar cells found in all the mutant animals studied.

(E and F) Electron micrographs of the basolateral portions of typical acinar cells from wild-type and *Perk*−/− mice. Note the presence of a distended and fragmented ER and the increased density of the ER content in the mutant, (F). The horizontal bars correspond to 1 μm in (A), (B), and (D–F), and to 200 nm in (C).

PERK phosphorylates eIF2α and attenuates translation in response to stress signals generated by protein malfolding in the ER lumen (Harding et al., 1999; Bertolotti et al., 2000; Sood et al., 2000). The fraction of phosphorylated eIF2α that can be attributed to PERK activity is highest in the pancreas (Figure 1D). PERK's absence leads to increased activity of a parallel stress pathway mediated by IRE1α (Figure 1E). These findings suggest that under physiological conditions, PERK insures that production and translocation of newly synthesized polypeptides into the lumen of ER will not exceed the capacity of the organelle to fold and process them. In the absence of PERK, the physiological signals that promote protein synthesis are unchecked and ER stress develops with deleterious effects on cell survival. According to this model, the specialization of pancreatic cells for protein secretion and the heavy physiological load placed on their rough ER explain the conspicuous consequences of the mutation. Both the functional reserve and regenerative capacity of tissues is likely to play an important role in a degenerative phenotype such as that of the *Perk*−/− mice. It is possible, therefore, that other cells that are active in protein secretion are also affected by the mutation, but that the phenotypic consequences are most obvious in the endocrine and exocrine portions of the pancreas.

The proposed interplay between physiological load and PERK activity is also consistent with our analysis of the endocrine pancreas. β cells in the islets of Langerhans respond to a switch from low glucose to high glucose by increasing insulin mRNA translation (Itoh and Okamoto, 1980; Welsh et al., 1986; Skelly et al., 1996). The glucose-mediated increase in insulin biosynthesis was more pronounced in *Perk*−/− islets than in wild-type islets. This suggests that under physiological conditions, PERK moderates translation in response to glucose-mediated signals that otherwise promote insulin synthesis, limiting the load placed on the cell's ER. Following the ingestion of carbohydrates, mutant mice would therefore be expected to experience higher loads on their β cell ER and higher levels of ER stress. Despite this defect in translational control, ER function measured in terms of proinsulin processing is preserved for some time in the *Perk*−/− β cells.

The switch from low to high glucose is associated with increased activity of the eIF2B guanine nucleotide exchange factor in islets (Gilligan et al., 1996). *Perk*−/− islets had no detectable defect in repressing insulin translation at physiologically low glucose levels (Figure 4A), indicating that *Perk* is not essential for the repression of eIF2B activity observed under such conditions. Furthermore, we found that in the glucose-responsive INS-1 islet cell line, PERK was more inducible by agents that cause ER stress when cells were cultured at 16.7 mM glucose than at 2.8 mM glucose (data not shown). These results indicate that PERK is important to islet

homeostasis under conditions of physiological demand and not for maintaining quiescence in the fasted state. The culture of cells in media totally lacking glucose readily activates PERK and other ER stress transducers (data not shown) and induces the UPR (Lee, 1987). It is doubtful, however, that translational regulation in cells cultured in media with no glucose is relevant to the physiology of β cells.

The most striking feature of the affected tissues in the *Perk*−/− animals was the extensive death of endocrine and exocrine pancreatic cells. In the endocrine pancreas, this led to the progressive replacement of the insulin-producing β cells with glucagon-producing α cells. This pattern is, however, not specific to the *Perk* mutation, and likely reflects the stereotyped response of the tissue to damage of any cause (Teitelman et al., 1993, Teitelman, 1996). As the *Perk*−/− mice aged, we observed a close correlation between the loss of β cell mass and the development of hyperglycemia. Nonetheless, we cannot exclude a functional defect in *Perk*−/− β cells that might also contribute to hyperglycemia. A functional defect, if it exists, is even more likely to play a role in the mild and nonprogressive glucose intolerance of the *Perk*+/− mice, which had less cell death in their islets than *Perk*−/− animals and normal-appearing islets of Langerhans (Figure 3C and data not shown).

Ultrastructural analysis of the *Perk*−/− pancreas revealed striking changes in the morphology of the ER. In the acinar cells, dilation, accumulation of electron-dense material in the lumen, and segmentation of the ER were commonly observed. Most islet cells in prediabetic *Perk*−/− mice were, by contrast, morphologically normal. However, a small subpopulation of islet cells with remarkable dilation of the ER lumen and accumulation of large quantities of electron-dense material were observed in all mutant animals and in none of the wild-type. We speculate that the islet cells in *Perk*−/− animals can compensate for the lack of translational control, and that these compensatory mechanisms allow the ER to maintain its function for some time. Indeed, pulse-chase labeling experiments reveal that ER processing of proinsulin is normal in the bulk of *Perk*−/− β cells, and that insulin secretion in response to glucose by mutant islets cultured in vitro is likewise preserved (Figures 4B and 4C, and data not shown). Eventually, the physiological demands on the β cell exhaust the capacity of these putative compensatory mechanisms. According to this speculation, the occasional cells with massively dilated ER reflect the consequences of such decompensation. The infrequency with which such cells are observed is possibly due to their dying soon after entering this presumably decompensated state. Increased activity of IRE1 observed in the pancreas of *Perk*−/− mice may promote programmed cell death (Wang et al., 1998b), and induction of JNK, mediated by IRE1 (Urano et al., 2000), may be an important link in this process.

The model proposed above for the pathophysiology of secretory cell dysfunction and death in *Perk*−/− mice emphasizes the role of translational regulation in preventing ER stress. However, we have recently found that PERK-mediated phosphorylation of eIF2α and translational regulation also control the activity of a signaling pathway that culminates in the increased expression of the genes *ATF4*, *CHOP*, and *BiP* (Harding et al., 2000a). Mice lacking *ATF4* have no reported defects in glycemic control (Tanaka et al., 1998; Hettmann et al., 2000). However, BiP expression has been reported to protect cells against the deleterious effects of ER stress (Lowenstein et al., 1991; Koong et al., 1994; Morris et al., 1997), and while CHOP promotes apoptosis of cells damaged by ER stress (Zinszner et al., 1998), it may also control the expression of downstream genes with a role in cellular regeneration (Wang et al., 1998a). Therefore, defective activation of specific stress-responsive genes may contribute to the phenotype of *Perk*−/− mice.

Inability to induce stress-responsive genes that are regulated by other eIF2α kinases (such as GCN2) may explain some of the differences in the phenotype between *Perk*−/− and mice bearing a point mutation replacing Ser51 of eIF2α with alanine (eIF2$\alpha^{Ser51Ala}$). In the latter, neonatal hypoglycemia predominates, possibly a consequence of the inadequate induction of genes encoding gluconeogenic enzymes. In addition, the islets of Langerhans of the eIF2$\alpha^{Ser51Ala}$ mutant mice are abnormal at birth, suggesting a developmental role for eIF2α phosphorylation that can proceed in the absence of *PERK* (Scheuner et al., 2001 [this issue of *Molecular Cell*]).

The phenotype of the *Perk*−/− mice is very similar to that observed in humans suffering from the Wolcott-Rallison syndrome, the consistent feature of which is severe diabetes mellitus developing in infancy (Wolcott and Rallison, 1972; Thornton et al., 1997). Mutations in the human PERK-encoding *EIF2AK3* gene have recently been reported in two families with the syndrome; however, the pathophysiological basis for the phenotype was not addressed (Delepine et al., 2000). Perhaps the special sensitivity of insulin-producing cells to a mutation that affects a signaling protein responsive to ER stress may also be relevant to the development of more common forms of human diabetes mellitus. The major abnormality in most patients with the common, type II form of the disease is peripheral resistance to the action of insulin. However, glucose intolerance develops only after β cell decompensation renders the endocrine pancreas unable to keep up with the demand imposed by insulin resistance (Porte, 1999; Cavaghan et al., 2000). We propose that over time, chronic ER stress might contribute to the attrition of β cell function and mass observed in many cases of type II diabetes mellitus. According to this speculation, the mutation we created in *Perk* artificially accelerates a process that is played out over many years in the endocrine pancreas of patients with type II diabetes mellitus.

Experimental Procedures

Perk Mutant Mice

The genomic region encoding the PERK transmembrane domain was replaced in embryonic stem cells using a neomycin resistance replacement cassette, yielding a null allele (Harding et al., 2000b). Two correctly targeted heterozygote embryonic stem cell clones were injected into C57BL/6 blastocysts, and chimeric males that transmitted the mutant allele through their germline were obtained from both lines. Animals were genotyped by PCR using three primers: 1740S (5′-AAG GAC CCT ATC CTC CTG CTG CAC-3′, which anneals in the deleted region), PGK.255R (5′-GCT ACC GGT GGA TGT GGA ATG TG-3′, which anneals at the inserted PGK.Neo^r cassette), and i.6AS (5′-CGG AGA CAG TAC AAG CGC AGA TGA-3′,

which anneals in an intronic sequence located in the 3′ homology arm). The wild-type allele and targeted allele give bands of 231 and 302 bp, respectively.

All experimental procedures involving mice were approved by the NYU School of Medicine's IACUC. Mice were maintained in a specific pathogen-free facility with a 12 hr light/dark cycle and unlimited access to food and water. The *Perk* mutation was maintained in two different genetic backgrounds: inbred 129svev and backcross into the outbred Swiss Webster strain. In the inbred strain, *Perk*−/− mice died in the first few days of life, and in the (129svev;Swiss Webster) F2 hybrid background, about half of the expected number of *Perk*−/− mice were recovered at weaning. In all studies comparing *Perk*+/+ and *Perk*−/− mice, we used sex-matched siblings derived from matings of *Perk*+/− animals in a (129svev;Swiss Webster) F2 background. Because the *Perk*−/− pups are distinguishable from +/+ and +/− littermates by their reduced size by day 3 of life, we routinely increase the recovery of *Perk*−/− animals born in large litters by removing some normal-sized offspring. To compare *Perk*+/− and *Perk*+/+ animals, we used isogenic 129svev mice.

Blood Glucose and Insulin Measurements and Detection of Steatorrhea

Blood glucose levels were measured with a portable glucose measuring device (Accu-Check). Insulin levels in serum were measured by ELISA, using mouse insulin as a standard (Crystal Chem). Intraperitoneal glucose tolerance tests were performed on 6-month-old *Perk*+/+ and *Perk*+/− animals that had been fasted for 20 hr. Animals were injected intraperitoneally with 2 mg/g body weight glucose, and blood glucose levels were determined at intervals thereafter.

Fat malabsorption (steatorrhea) was detected by switching 35-day-old *Perk*−/− and *Perk*+/+ littermates (n = 4 each) that had been maintained on a normal lab chow to a 45% fat diet (Research Diets). Aliquots of fresh stool samples collected for 6 hr periods on 2 consecutive days were homogenized after adding water at 10 μl/mg stool. After centrifugation at 200 g for 5 min to remove insoluble material, 5 μl of the supernatant was applied to a gelatin-coated glass slide and mixed by pipeting with 5 μl freshly diluted and filtered Oil Red O stain (40%). Duplicate slides were dried, and coverslips were mounted with 50% glycerol and examined by light microscopy.

Immunostaining, In Situ Histohybridization, TUNEL Assays, and BrdU Incorporation

Animals were killed by CO_2 asphyxiation and tissues were fixed by cardiac perfusion with 4% paraformaldehyde in PBS. Tissues were removed and fixed an additional 4–16 hr in the same solution at 4°C. After rinsing in PBS, tissues were either incubated overnight in 30% sucrose at 4°C (for frozen sections) or dehydrated through a graded series of ethanol, cleared in xylenes, and embedded in paraffin.

PERK immunoreactivity was detected using affinity-purified rabbit anti-murine PERK antiserum (Harding et al., 1999) diluted 1/300. Endogenous peroxidase activity in 5 μm paraffin sections was blocked by treating with 3% H_2O_2 in PBS. Primary antibody incubation was followed by 1/200 diluted biotinylated goat anti-rabbit (Jackson Labs) and avidin-biotin-HRP complex (Vector ABC kit).

Insulin and glucagon immunoreactivity were detected by incubating 5 μm frozen sections of mouse pancreas with a guinea pig anti-bovine insulin (Linco) diluted 1/4000 and rabbit anti-glucagon (Zymed) diluted 1/500, followed by incubation with biotinylated goat anti-guinea pig and then streptavidin-DTAF and Texas red-conjugated goat anti-rabbit (all from Jackson Labs) diluted to 1/200. Slides were mounted in a fluoro-protective aqueous mounting medium (Citifluor, Ted Pella).

Insulin mRNA was detected by in situ histohybridization using a digoxigenin-labeled antisense RNA probe (DIG-RNA labeling kit; Roche) synthesized from the cloned 326 bp HindIII-PvuII fragment from the mouse insulin II gene. Fresh cut 8 μm frozen pancreas sections were dried and fixed onto slides in 4% paraformaldehyde, digested with proteinase K, and hybridized overnight at 55°C with 1 μg/ml labeled probe in 50% formamide, 10% dextran sulfate, 1% Denhardt's, 250 μg/ml yeast tRNA, 0.3 M NaCl, 20 mM Tris-HCl (pH 8), 5 mM EDTA, 10 mM $NaPO_4$, and 1% sarcosyl. After hybridization sections were washed in 50% formamide 2× SSC at 65°C they were digested with RNase A, blocked with 10% normal goat serum for 1 hr, and incubated with alkaline phosphatase-coupled anti-digoxigenin antibody and developed using BM purple (according to the manufacturer's instructions; Roche).

TUNEL assays were performed on paraffin sections using the fluorescein-apoptosis detection kit from Promega according to the manufacturer's instructions.

BrdU labeling, 10 hr after intraperitoneal injection of mice with 0.1 mg/g BrdU solution, was detected in deparaffinized sections using a kit (Amersham). Photomicrographs were obtained with a SPOT digital camera system mounted on a Zeiss Axiophot-100 microscope.

Immunoprecipitation and Western Analysis

Tissues were removed and rinsed in ice cold PBS, and then immediately homogenized in five volumes of Triton X-100 buffer (20 mM HEPES [pH 7.5], 150 mM NaCl, 1% Triton X-100, 10% glycerol, 1 mM EDTA, 10 mM tetrasodium pyrophosphate, 100 mM NaF, 17.5 mM β-glycerophosphate, 10 mM phenylmethylsulfonyl fluoride, 15 μg/ml aprotonin, and 6 μg/ml pepstatin A) using a motorized teflon and glass homogenizer. After incubation on ice for 15 min, the extracts were cleared by centrifugation at 14,000 rpm twice for 30 min each. The protein content of each extract was determined by Bradford assay. The extracts (6 mg per sample for Figure 1B or 1.6 mg of protein for Figures 1C and 1E) were precleared by incubation with 2 μl of nonimmune serum and 15 μl of protein A sepharose for 1 hr at 4°C. PERK, IRE1α, or GCN2 were then immunoprecipitated overnight with 1.5 μl of each specific antiserum (Harding et al., 1999, 2000a; Urano et al., 2000) and 15 μl of protein A sepharose. Proteins from the RIPA-washed immunoprecipitates were separated by 7.5% SDS-PAGE and transferred to nitrocellulose. For eIF2α and BiP Westerns, 45 μg of cleared extract was separated by 10% SDS-PAGE and the proteins were transferred to nitrocellulose. Immunoblot analysis using polyclonal anti−PERK (1/5000), anti-phospho-PERK (1/5000), anti-IRE1α (1/2000), anti-GCN2 (1/3000), anti-BiP (1/3000, a gift of Gert Kreibich), anti-phospho-eIF2α, or a monoclonal anti-eIF2α antibody that detects all forms of the protein (Scorsone et al., 1987) were performed as previously described (Harding et al., 2000b).

Islets of Langerhans Isolation and Metabolic Labeling

Islets from 12-day-old *Perk*+/+ or *Perk*−/− mice were handpicked from collagenase P-digested whole pancreas (Lacy and Kostianovsky, 1967). Freshly isolated islets (80 size-matched *Perk*+/+ or *Perk*−/− islets per experimental point) were cultured for 14 hr in RPMI 10% FCS (conditions known to maintain glucose-induced insulin biosynthesis; Andersson, 1978). Glucose-induced insulin biosynthesis was analyzed following established methods (Welsh et al., 1986; Skelly et al., 1998). Briefly, islets were washed three times in 1 ml of Kreb's Ringer-bicarbonate buffer (115 mM NaCl, 5 mM KCl, 10 mM $NaHCO_3$, 2.5 mM $MgCl_2$, 2.5 mM $CaCl_2$, and 20 mM HEPES [pH 7.4]) containing 0.1% BSA, and then incubated in 300 μl of the same buffer containing 2.8 mM glucose for 1 hr at 37°C. The buffer was removed by centrifugation, and 200 μl of new buffer containing either 2.8 or 16.7 mM glucose was added and the incubation was continued for 1 hr. During the final 20 min of incubation, 50 μCi of [^{35}S]Met-Cys TransLabel (ICN) was added to each sample. For the pulse-chase experiments, the islets were cultured in 16.7 mM glucose for 40 min, pulsed in the same for 20 min as above, and chased in the presence of unlabeled methionine (0.6 mg/ml) and cysteine (0.96 mg/ml). The media was removed and the islets were lysed on ice in 300 μl of Triton buffer. The lysate was cleared by centrifugation at 14,000 rpm for 15 min at 4°C and proinsulin was immunoprecipitated with 1 μl of anti-rat insulin-C peptide antiserum (Linco). Immunoprecipitated proteins were resolved on a 15% tricine-urea acrylamide gel (Schagger and von Jagow, 1987). The incorporation of [^{35}S]Met or Cys into proinsulin was quantified by exposing the fixed dried gels exposed to a phosphor-screen using IMAGE-Quant software (Molecular Dynamics).

Acknowledgments

We thank G. Holz and M. Hussein for advice on islet physiology, isolation, and culture, P. Arora for help in detecting steatorrhea, A.

Auerbach and M.J. Sunshine for producing chimeric mice, and E.Y. Skolnik, R. Kaufman, and A. Bertolotti for valuable discussions. Supported by NIH grants (ES08681 and DK47119). H.P.H. was supported by an NRSA grant (F32-CA73181). D.R. is a scholar of the Leukemia and Lymphoma Society of America and a recipient of an Ellison Medical Foundation Senior Scholars Award.

Received November 2, 2000; revised February 22, 2001.

References

Andersson, A. (1978). Isolated mouse pancreatic islets in culture: effects of serum and different culture media on the insulin production of the islets. Diabetologia *14*, 397–404.

Bertolotti, A., Zhang, Y., Hendershot, L., Harding, H., and Ron, D. (2000). Dynamic interaction of BiP and the ER stress transducers in the unfolded protein response. Nat. Cell Biol. *2*, 326–332.

Cavaghan, M.K., Ehrmann, D.A., and Polonsky, K.S. (2000). Interactions between insulin resistance and insulin secretion in the development of glucose intolerance. J. Clin. Invest. *106*, 329–333.

Clemens, M. (1996). Protein kinases that phosphorylate eIF2 and eIF2B, their role in eukaryotic cell translational control. In Translational Control, J. Hershey, M. Mathews, and N. Sonenberg, eds. (Cold Spring Harbor, NY: Cold Spring Harbor Laboratory Press), pp. 139–172.

Delepine, M., Nicolino, M., Barrett, T., Golamaully, M., Lathrop, G.M., and Julier, C. (2000). EIF2AK3, encoding translation initiation factor 2-alpha kinase *3*, is mutated in patients with Wolcott-Rallison syndrome. Nat. Genet. *25*, 406–409.

Gilligan, M., Welsh, G.I., Flynn, A., Bujalska, I., Diggle, T.A., Denton, R.M., Proud, C.G., and Docherty, K. (1996). Glucose stimulates the activity of the guanine nucleotide-exchange factor eIF-2B in isolated rat islets of Langerhans. J. Biol. Chem. *271*, 2121–2125.

Harding, H., Zhang, Y., and Ron, D. (1999). Translation and protein folding are coupled by an endoplasmic reticulum resident kinase. Nature *397*, 271–274.

Harding, H., Novoa, I., Zhang, Y., Zeng, H., Wek, R.C., Schapira, M., and Ron, D. (2000a). Regulated translation initiation controls stress-induced gene expression in mammalian cells. Mol. Cell *6*, 1099–1108.

Harding, H., Zhang, Y., Bertolotti, A., Zeng, H., and Ron, D. (2000b). *Perk* is essential for translational regulation and cell survival during the unfolded protein response. Mol. Cell *5*, 897–904.

Hettmann, T., Barton, K., and Leiden, J.M. (2000). Microphthalmia due to p53-mediated apoptosis of anterior lens epithelial cells in mice lacking the CREB-2 transcription factor. Dev. Biol. *222*, 110–123.

Itoh, N., and Okamoto, H. (1980). Translational control of proinsulin synthesis by glucose. Nature *283*, 100–102.

Kaufman, R.J. (1999). Stress signaling from the lumen of the endoplasmic reticulum: coordination of gene transcriptional and translational controls. Genes Dev. *13*, 1211–1233.

Kimball, S.R., and Jefferson, L.S. (1992). Regulation of protein synthesis by modulation of intracellular calcium in rat liver. Am. J. Physiol. *263*, E958–E964.

Koong, A.C., Chen, E.Y., Lee, A.S., Brown, J.M., and Giaccia, A.J. (1994). Increased cytotoxicity of chronic hypoxic cells by molecular inhibition of GRP78 induction. Int. J. Radiat. Oncol. Biol. Phys. *28*, 661–666.

Lacy, P.E., and Kostianovsky, M. (1967). Method for the isolation of intact islets of Langerhans from the rat pancreas. Diabetes *16*, 35–39.

Lee, A.S. (1987). Coordinate regulation of a set of genes by glucose and calcium ionophores in mammalian cells. Trends Biochem. Sci. *12*, 20–23.

Liu, C.Y., Schroder, M., and Kaufman, R.J. (2000). Ligand-independent dimerization activates the stress-response kinases IRE1 and PERK in the lumen of the endoplasmic reticulum. J. Biol. Chem. *275*, 24881–24885.

Lowenstein, D., Chan, P., and Miles, M. (1991). The stress protein response in cultured neurons: characterization and evidence for a protective role in excitotoxicity. Neuron *7*, 1053–1060.

Mori, K. (2000). Tripartite management of unfolded proteins in the endoplasmic reticulum. Cell *101*, 451–454.

Morris, J.A., Dorner, A.J., Edwards, C.A., Hendershot, L.M., and Kaufman, R.J. (1997). Immunoglobulin binding protein (BiP) function is required to protect cells from endoplasmic reticulum stress but is not required for the secretion of selective proteins. J. Biol. Chem. *272*, 4327–4334.

Pictet, R.L., Clark, W.R., Williams, R.H., and Rutter, W.J. (1972). An ultrastructural analysis of the developing embryonic pancreas. Dev. Biol. *29*, 436–467.

Porte, D., Jr. (1999). Mechanisms for hyperglycemia in the metabolic syndrome. The key role of β-cell dysfunction. Ann. N Y Acad. Sci. *892*, 73–83.

Prostko, C.R., Brostrom, M.A., Malara, E.M., and Brostrom, C.O. (1992). Phosphorylation of eukaryotic initiation factor (eIF) 2 α and inhibition of eIF-2B in GH3 pituitary cells by perturbants of early protein processing that induce GRP78. J. Biol. Chem. *267*, 16751–16754.

Prostko, C.R., Brostrom, M.A., and Brostrom, C.O. (1993). Reversible phosphorylation of eukaryotic initiation factor 2 α in response to endoplasmic reticular signaling. Mol. Cell. Biochem. *127–128*, 255–265.

Schagger, H., and von Jagow, G. (1987). Tricine-sodium dodecyl sulfate-polyacrylamide gel electrophoresis for the separation of proteins in the range from 1 to 100 kDa. Anal. Biochem. *166*, 368–379.

Scheuner, D., Song, B., McEwen, E., Liu, C., Laybutt, R., Gillespie, P., Saunders, T., Bonner-Weir, S., and Kaufman, R.J. (2001). Translational control is required for the unfolded protein response and in vivo glucose homeostasis. Mol. Cell *7*, this issue, 1165–1176.

Scorsone, K.A., Panniers, R., Rowlands, A.G., and Henshaw, E.C. (1987). Phosphorylation of eukaryotic initiation factor 2 during physiological stresses which affect protein synthesis. J. Biol. Chem. *262*, 14538–14543.

Shi, Y., Vattem, K.M., Sood, R., An, J., Liang, J., Stramm, L., and Wek, R.C. (1998). Identification and characterization of pancreatic eukaryotic initiation factor 2 α-subunit kinase, PEK, involved in translational control. Mol. Cell. Biol. *18*, 7499–7509.

Skelly, R.H., Schuppin, G.T., Ishihara, H., Oka, Y., and Rhodes, C.J. (1996). Glucose-regulated translational control of proinsulin biosynthesis with that of the proinsulin endopeptidases PC2 and PC3 in the insulin- producing MIN6 cell line. Diabetes *45*, 37–43.

Skelly, R.H., Bollheimer, L.C., Wicksteed, B.L., Corkey, B.E., and Rhodes, C.J. (1998). A distinct difference in the metabolic stimulus-response coupling pathways for regulating proinsulin biosynthesis and insulin secretion that lies at the level of a requirement for fatty acyl moieties. Biochem. J. *331*, 553–561.

Sood, R., Porter, A.C., Ma, K., Quilliam, L.A., and Wek, R.C. (2000). Pancreatic eukaryotic initiation factor-2α kinase (PEK) homologues in humans, *Drosophila melanogaster* and *Caenorhabditis elegans* that mediate translational control in response to endoplasmic reticulum stress. Biochem. J. *346 Pt 2*, 281–293.

Tanaka, T., Tsujimura, T., Takeda, K., Sugihara, A., Maekawa, A., Terada, N., Yoshida, N., and Akira, S. (1998). Targeted disruption of ATF4 discloses its essential role in the formation of eye lens fibres. Genes Cells *3*, 801–810.

Teitelman, G. (1996). Induction of β-cell neogenesis by islet injury. Diabetes Metab. Rev. *12*, 91–102.

Teitelman, G., Alpert, S., Polak, J.M., Martinez, A., and Hanahan, D. (1993). Precursor cells of mouse endocrine pancreas coexpress insulin, glucagon and the neuronal proteins tyrosine hydroxylase and neuropeptide Y, but not pancreatic polypeptide. Development *118*, 1031–1039.

Thornton, C.M., Carson, D.J., and Stewart, F.J. (1997). Autopsy findings in the Wolcott-Rallison syndrome. Pediatr. Pathol. Lab. Med. *17*, 487–496.

Tirasophon, W., Welihinda, A.A., and Kaufman, R.J. (1998). A stress

response pathway from the endoplasmic reticulum to the nucleus requires a novel bifunctional protein kinase/endoribonuclease (Ire1p) in mammalian cells. Genes Dev. *12*, 1812–1824.

Urano, F., Wang, X., Bertolotti, A., Zhang, Y., Chung, P., Harding, H., and Ron, D. (2000). Coupling of stress in the endoplasmic reticulum to activation of JNK protein kinases by transmembrane protein kinase IRE1. Science *287*, 664–666.

Wang, X.-Z., Kuroda, M., Sok, J., Batchvarova, N., Kimmel, R., Chung, P., Zinszner, H., and Ron, D. (1998a). Identification of novel stress-induced genes downstream of chop. EMBO J. *17*, 3619–3630.

Wang, X.Z., Harding, H.P., Zhang, Y., Jolicoeur, E.M., Kuroda, M., and Ron, D. (1998b). Cloning of mammalian Ire1 reveals diversity in the ER stress responses. EMBO J. *17*, 5708–5717.

Welsh, M., Scherberg, N., Gilmore, R., and Steiner, D.F. (1986). Translational control of insulin biosynthesis. Evidence for regulation of elongation, initiation and signal-recognition-particle-mediated translational arrest by glucose. Biochem. J. *235*, 459–467.

Wolcott, C., and Rallison, M. (1972). Infancy-onset diabetes mellitus and multiple epiphyseal dysplasia. J. Pediatr. *80*, 292–297.

Zinszner, H., Kuroda, M., Wang, X., Batchvarova, N., Lightfoot, R.T., Remotti, H., Stevens, J.L., and Ron, D. (1998). CHOP is implicated in programmed cell death in response to impaired function of the endoplasmic reticulum. Genes Dev. *12*, 982–995.

PERSPECTIVES: PROTEIN SYNTHESIS

The Perks of Balancing Glucose

Nahum Sonenberg and Christopher B. Newgard

Development, differentiation, and growth of eukaryotic cells can be regulated by modulating the translation of mRNAs into proteins. Many signaling pathways regulate mRNA translation and protein synthesis, and perturbations in these pathways can result in metabolic dysregulation and disease. Two recent reports in *Molecular Cell* by Harding *et al.* (*1*) and Scheuner *et al*. (*2*) now tie together translational regulation and glucose metabolism. Both groups show in genetically engineered mice that a protein kinase that phosphorylates a master regulator of translation—eukaryotic translation initiation factor–2 (eIF2)—promotes the survival of insulin-secreting pancreatic β cells, thus contributing to glucose homeostasis.

Genetic and biochemical analyses of the yeast *Saccharomyces cerevisiae* (*3*) has shown that a single known kinase, Gcn2p, that phosphorylates the α subunit of eIF2, leading to inhibition of protein synthesis. Gcn2p itself is activated by uncharged transfer RNAs (tRNAs without attached amino acids) under starvation conditions when the amino acid pool is depleted. Paradoxically, synthesis of the transcription factor Gcn4p is enhanced in response to activation of Gcn2p and phosphorylation of eIF2α (*3*). Gcn4p switches on expression of genes encoding enzymes that make amino acids. Thus, in yeast, phosphorylation of eIF2α serves predominantly to regulate gene expression at the transcriptional level in response to nutritional deprivation.

In eukaryotes, translational control operates primarily during the first steps of translation when the small (40*S*) ribosomal subunit, charged with an initiator tRNA, is recruited to the 5′ end of mRNA. Initiation of translation is modulated in part by the activity of the eIF4F complex that recognizes the modified 5′ end of mRNA, and in part by eIF2, which recruits the charged initiator tRNA to the 40*S* ribosomal subunit. Phosphorylation of a serine at position 51 (Ser^{51}) in the α subunit of eIF2 is crucial for preventing this step and for halting protein synthesis. When phosphorylated, eIF2 inhibits the guanine nucleotide exchange factor eIF2B, becoming trapped in its inactive (guanosine diphosphate–bound) form and unable to initiate translation (*3*).

Four distinct kinases are known to phosphorylate eIF2α on Ser^{51} in mammals. Each is activated by specific signals that elicit translational control in response to distinct needs. RNA-activated protein kinase is activated by double-stranded RNA produced during viral infection and halts protein synthesis, thus preventing production of viral proteins. Heme-regulated inhibitor kinase is activated when heme concentrations in maturing red blood cells become too low, switching off synthesis of globin. Perturbed protein folding in the endoplasmic reticulum (ER) induces eIF2α phosphorylation and the attenuation of protein synthesis (see the figure) (*4*). The kinase responsible for this unfolded protein response is PERK (*5*). Identified as the eIF2 kinase enriched in pancreatic cells (*6*), PERK is a transmembrane protein resident in the ER membrane whose activity is repressed by the ER chaperone BiP. When too many unfolded proteins accumulate in the ER, BiP dissociates from PERK, resulting in the activation of this kinase, which then phosphorylates eIF2α (*7, 8*). Through halting translation initiation and protein synthesis, PERK may relieve ER stress by reducing the number of unfolded proteins in the ER (*9, 10*).

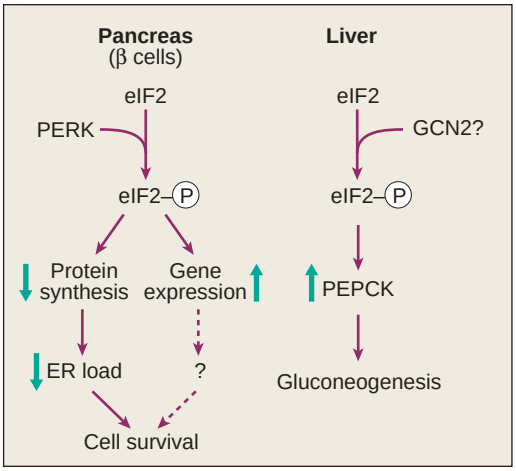

Perking up protein synthesis. (Left) Phosphorylation of eIF2α by PERK in response to unfolded proteins in the ER inhibits translation initiation and protein synthesis in pancreatic β cells. This results in a decrease in the number of unfolded proteins in the ER and promotion of β cell survival. eIF2α phosphorylation also results in the transcriptional activation of genes that are important for cell survival. **(Right)** Control of glucose production (gluconeogenesis) in the liver by eIF2α phosphorylation may be mediated by GCN2 because deletion of the other eIF2α kinases (including PERK) does not result in hypoglycemia. eIF2α phosphorylation may increase the synthesis of gluconeogenic enzymes (such as PEPCK) or of transcription factors that activate the expression of their genes.

By engineering PERK-deficient mice (*1*) or mice with a mutation in the eIF2α phosphorylation site ($Ser^{51} \rightarrow$ Ala) (*2*), Harding, Scheuner, and their colleagues reveal that eIF2α phosphorylation is connected to glucose metabolism. The PERK-deficient and Ser^{51} mutant mice exhibited severe but opposing defects in glucose homeostasis. PERK-deficient animals developed marked hyperglycemia (elevated blood glucose) at 4 weeks of age, whereas the Ser^{51} mutant mice were normal at birth but died of severe hypoglycemia 18 hours later. Both mutant strains had defects in pancreatic β cells; these defects were apparent in Ser^{51} mutant embryos, but only became apparent in PERK-deficient animals several weeks after birth.

The difference between the two animal models suggests that more than one type of eIF2 kinase may be operating in the insulin-producing β cells of the pancreas. A feature common to both mouse models is the decrease (but not complete absence) of β cells, large numbers of which undergo apoptosis in the PERK-deficient mice (*11*). That the loss of β cells appears in the setting of hyperglycemia in one model and hypoglycemia in the other implies that this β cell insufficiency is directly caused by loss of normal eIF2α-mediated translational control and is not a secondary effect in response to disruption of glucose homeostasis.

The fatal hypoglycemia in the Ser^{51} mutant mice may be caused by defects in glucose production in the liver (gluconeogenesis). In utero, the fetus is supplied with ample amounts of glucose through the placental circulation. At birth, this source of glucose is extinguished and the newborn mammal must activate enzymes that promote the conversion of gluconeogenesis precursors to glucose. The induction of this gluconeogenesis program is defective in the eIF2α mutant mice, as reflected by their failure to increase the amount of the gluconeogenic enzyme phosphoenol-pyruvate carboxykinase (PEPCK). Intriguingly, synthesis of one of the transcription factors that induces expression of the *PEPCK* gene is regulated by eIF2α phosphorylation. It will thus be important to determine whether loss of eIF2α phosphorylation decreases synthesis of this transcription factor in the liver cells of mutant mice. Phosphorylation of eIF2α is clearly

N. Sonenberg is in the Department of Biochemistry and McGill Cancer Center, McGill University, Montreal, Quebec H3G 1Y6, Canada. C. B. Newgard is in the Department of Biochemistry and the Touchstone Center for Diabetes Research, University of Texas Southwestern Medical Center, Dallas, TX 75390, USA.

important for regulation of PEPCK expression. Any broad conclusions, however, must await further studies on other key gluconeogenic enzyme genes and their expression in response to perturbations other than birth, such as fasting and refeeding.

Why is it that mice with defective eIF2α phosphorylation exhibit both β cell insufficiency and defective liver gluconeogenesis, whereas PERK-deficient animals only exhibit β cell insufficiency? The Harding *et al*. work (*1*) provides a possible answer: PERK-deficient mice have a reduced ratio of phosphorylated to total eIF2α in pancreas, lung, and thymus, but a normal ratio in liver and spleen. This finding suggests that an eIF2α kinase other than PERK may be the key modulator of translational control of gluconeogenic enzyme expression in the liver. If eIF2α phosphorylation does prove to be important in this pathway, the mammalian homolog of yeast *GCN2* (which is activated by amino acid deprivation) may be involved (see the figure). Defective gene expression downstream of GCN2, however, is unlikely to account for all of the characteristics of the eIF2 mutant mice, given that *GCN2*-deficient animals do not manifest any impairment in neonatal survival (*12*).

The importance of the new mouse models is underscored by the discovery of mutations in the *PERK* gene in an inherited autosomal recessive disease in humans, called the Wolcott-Rallison syndrome (*13*). This disease is classified as a form of type 1 diabetes because it develops in early infancy and is characterized by the destruction of pancreatic β cells. A key question posed by the Harding and Scheuner studies is why β cells are selectively destroyed in Wolcott-Rallison patients and in the mutant mice. It is very likely that β cells die because they need both PERK (which is extraordinarily abundant in the pancreas) and eIF2α phosphorylation to survive.

In yeast, eIF2α is phosphorylated in response to nutritional cues and directs adaptations in intermediary metabolism. The new work suggests that, despite considerable diversification in upstream signals, metazoans have retained the kinases that phosphorylate eIF2α and control translation, adapting them for the regulation of glucose homeostasis.

References

1. H. Harding *et al.*, *Mol. Cell* **7**, 1153 (2001).
2. D. Scheuner *et al.*, *Mol. Cell* **7**, 1165 (2001).
3. A. G. Hinnebusch, in *Translational Control of Gene Expression,* N. Sonenberg, J. W. B. Hershey, M. B. Mathews, Eds. (Cold Spring Harbor Laboratory Press, Cold Spring Harbor, NY, 2000), pp. 185–243.
4. C. R. Prostko *et al.*, *Mol. Cell. Biochem.* **127–128**, 255 (1993).
5. H. Harding *et al.*, *Nature* **397**, 271 (1999).
6. Y. Shi *et al.*, *J. Biol. Chem.* **274**, 5723 (1999).
7. A. Bertolotti *et al.*, *Nature Cell Biol.* **2**, 326 (2000).
8. C. Y. Liu *et al.*, *J. Biol. Chem.* **275**, 44881 (2000).
9. H. Harding *et al.*, *Mol. Cell* **5**, 897 (2000).
10. R. Sood *et al.*, *Biochem. J.* **346**, 281 (2000).
11. H. Harding *et al.*, *Mol. Cell* **6**, 1099 (2000).
12. D. Ron, personal communication.
13. M. Delepine *et al.*, *Nature Genet.* **25**, 406 (2000).